Diabetes, Metabolic Syndrome and Obesity

Dovepress
Taylor & Francis Group

Open Access Full Text Article

ORIGINAL RESEARCH

Obesity-Driven Segment-Specific Cerebrovascular Remodeling: A 3D High-Resolution Vessel Wall Imaging Study

Ai Li, Miao Yu, Qiang Lu, Fei Wang, Hongtao Niu*, Jun Zhang*

Medical Imaging Center, Qinhuangdao NO.1 Hospital, Qinhuangdao, Hebei, 066000, People's Republic of China

*These authors contributed equally to this work

Correspondence: Hongtao Niu; Jun Zhang, Medical Imaging Center, Qinhuangdao NO.1 Hospital, No. 258, Wenhua Road, Haigang District, Qinhuangdao, Hebei, 066000, People's Republic of China, Tel +86 323 128 6876, Email niuht2004@126.com; 507942009@qq.com

Purpose: This study aimed to compare differences in cerebrovascular luminal diameter (LD) and maximum wall thickness (MWT) among normal weight, overweight, and obese populations using three-dimensional high-resolution magnetic resonance vessel wall imaging (3D HRMR-VWI), and to evaluate the impact of body mass index (BMI, kg/m^2) on cerebrovascular structure.

Patients and Methods: Ninety-six subjects were categorized into normal weight, overweight, and obesity groups according to Chinese criteria. Two radiologists with more than five years of experience independently and blindly measured LD, MWT, and vessel wall status of the bilateral internal carotid artery (ICA) segments C1–C7 and the middle cerebral artery (MCA) M1 segments. Differences in LD, MWT, and vessel wall status among the three groups were analyzed.

Results: The right C3 segment LD in the overweight group was significantly larger than in the normal weight group (overweight: 4.245 ± 0.199 mm vs normal weight: 3.676 ± 0.412 mm (right); $p < 0.01$), while the obese group showed retraction (obesity: 3.969 ± 0.714 mm (right), $p < 0.01$). MWT increased significantly with higher BMI (Z=10.99, $\chi^2 = 122.89$, $P < 0.001$), with the most pronounced thickening in left C1, C2, and C6 segments in the obese group (H=19.806, 14.327, 21.732, $P < 0.001$). Each BMI increase (normal weight → overweight → obesity) raised the risk of vessel wall deterioration by 98% (OR=1.98, 95% CI: 1.75–2.24, $P < 0.001$).

Conclusion: 3D HRMR-VWI revealed segment-specific remodeling in obese individuals, confirming a dose–effect relationship between elevated BMI and vessel wall deterioration. This provides a basis for optimizing 3D HRMR-VWI screening (focusing on high-risk segments) and establishing BMI-stratified intervention thresholds.

Keywords: high-resolution magnetic resonance vessel wall imaging, obesity, cerebrovascular disease, stroke, atherosclerosis

Introduction

The global obesity epidemic correlates with rising cerebrovascular risks. According to WHO data, 2.5 billion adults were overweight in 2022, with over 890 million classified as obese (BMI ≥ 30 kg/m^2). Stroke, particularly ischemic stroke, remains a leading cause of mortality and disability worldwide.[1,2] Obesity accelerates atherosclerosis via mechanisms such as metabolic dysregulation, chronic inflammation, oxidative stress, and endothelial dysfunction, elevating stroke risk.[3–5]

Conventional cerebrovascular assessments include ultrasound (US), computed tomography angiography (CTA), magnetic resonance angiography (MRA), and digital subtraction angiography (DSA). US[6] detects hemodynamic changes but is limited to >50% stenosis screening. CTA[7] offers rapid spatial resolution but suffers from beam-hardening artifacts and radiation exposure. MRA[8] is non-invasive but poorly visualizes calcified plaques and small vessels. DSA[9] is the gold standard but invasive. These techniques primarily evaluate luminal abnormalities, failing to characterize non-stenotic vessel walls.[10] 3D HRMR-VWI[11–13] provides high-resolution visualization of intracranial/extracranial arterial walls, plaque components (fibrous cap, lipid core, hemorrhage), and early wall thickening, making it optimal for atherosclerosis assessment. 3D HRMR-VWI employs advanced black-blood sequences (eg, 3D Black-Blood FSE Cube T1WI) with isotropic high resolution (0.5×0.5×0.5 mm^3 voxels in this

https://doi.org/10.2147/DMSO.S564173
Received: 6 September 2025
Accepted: 16 February 2026
Published: 11 March 2026

study), which effectively suppresses intravascular blood signal while preserving the signal of arterial wall layers (intima, media, adventitia). This technique enables direct visualization of early wall thickening, plaque components (eg, lipid cores, fibrous caps), and structural remodeling without beam-hardening artifacts (CTA) or invasiveness (DSA). In neuroimaging, 3D HRMR-VWI[11–13] has become a cornerstone for detecting subclinical cerebrovascular atherosclerosis, as it can identify vascular changes before luminal stenosis develops—providing critical insights for stroke risk stratification in metabolic disorders.

Existing obesity-related studies focus on traditional risk factors (eg, lipids, blood pressure) or single segments (eg, carotid bifurcation). Few systematically combine 3D HRMR-VWI with the Bouthillier classification[14] to explore BMI-driven segment-specific remodeling. Precise segmental analysis is clinically vital for identifying early lesions. LD and MWT reflect critical pathology: stenosis indicates atherosclerosis, dissection, or moyamoya disease;[15–17] dilation suggests aneurysms;[18] wall thickening signals early arteriosclerosis or vasculitis.[19,20] Prior US/CTA studies were difficult to evaluate characteristics of full C1–C7 due to resolution limitations,[11] while 3D HRMR-VWI studies focused on severe stenosis,[13] neglecting subclinical obesity.

This study leveraged 3D HRMR-VWI to compare LD, MWT, and vessel wall status across ICA (C1–C7) and MCA (M1) segments in normal weight, overweight, and obese individuals during early metabolic dysregulation. We quantified BMI's impact on cerebrovascular structure and established a risk model for weight class-driven vessel wall deterioration.

Materials and Methods

Study Design and Population

This single-center cross-sectional study was conducted at Qinhuangdao NO.1 Hospital, a tertiary general hospital with specialized expertise in cerebrovascular imaging. Ninety-six subjects (aged 18–50) underwent 3D HRMR-VWI at our Hospital (January–May 2025). The study adhered to the *Declaration of Helsinki* and was approved by the Institutional Review Board (No. 2025K-250-01). Written informed consent was obtained.

Data Collection

Participants completed standardized questionnaires[21–23] covering demographics, lifestyle, medical history, physical/laboratory data (weight, height, blood pressure, sleep[24]). Fasting blood samples were analyzed for alanine aminotransferase (ALT), Aspartate aminotransferase (AST), γ-Glutamyl transpeptidase (GGT), Uric acid (UA), Creatinine (CR), Glucose (GLU), Total cholesterol (CHO), Low-density lipoprotein (LDL-C), High-density lipoprotein (HDL-C), Triglycerides (TG).

Inclusion Criteria

① Age 18–50; ② Ability to cooperate; ③ Stable weight (±<5% over 12 weeks); ④ Complete multimodal imaging and laboratory data.

Exclusion Criteria

① Use of anti-obesity drugs; ② History of bariatric surgery; ③ Hypertension or diabetes mellitus lasting>1 year;[25,26] ④ Arteritis, autoimmune disorders, dissection[27–29] or genetic obesity;[30–32] ⑤ MRI contraindications/poor image quality.

BMI stratification followed Chinese criteria:[33] normal weight (18.5–23.9 kg/m^2), overweight (24.0–27.9 kg/m^2), obesity (≥28.0 kg/m^2). The selection process of the final study population is illustrated in Figure 1.

MRI Protocol

Scanner: 3.0T GE Pioneer; Coil: 21-channel head-neck coil; Coverage: Aortic arch to centrum semiovale. Sequence: 3D Black-Blood FSE Cube T1WI.[34,35] Parameters: TR: 700 ms; TE: 10 ms; FOV: 200×200 mm; Matrix: 256×256; Slice thickness: 0.5 mm; Voxel size: 0.5×0.5×0.5 mm^3; NEX: 1; Acquisition time: 6 min 36s.

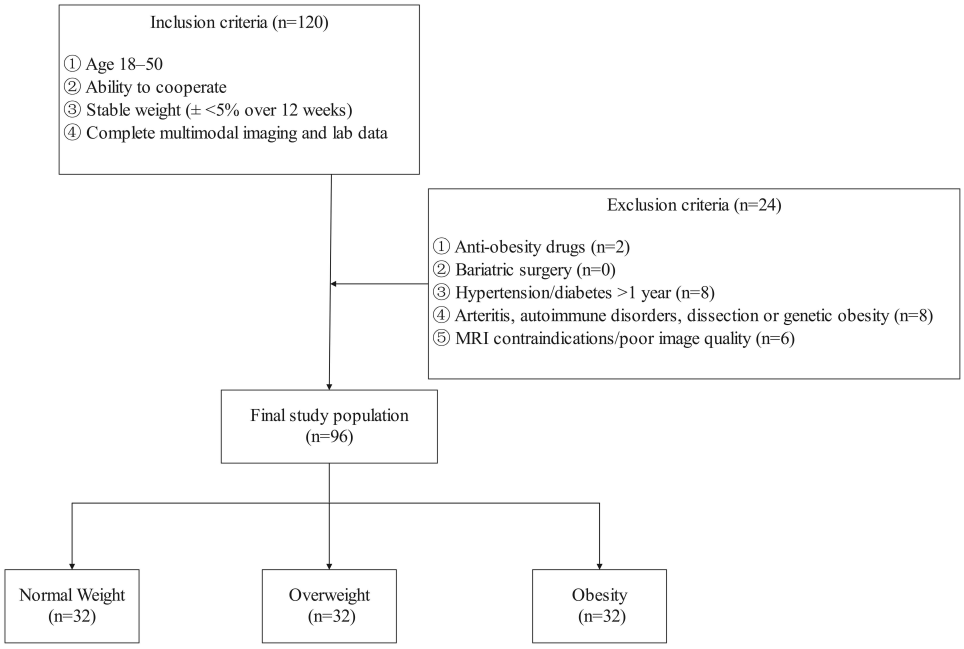

Figure 1 The flowchart of the selection process of participants.

Image Analysis

Based on the Bouthillier segmentation method, a total of 8 segments of the head and carotid arteries C1-C7 and M1 were analyzed synchronously with luminal-wall pairing, and all MR images were performed by two radiologists with more than five years of experience in neuroimaging diagnosis using Picture Archiving and Communication System (PACS) software and multiplanar recombination (MPR) post-processing technology,[36] maximum wall thickness (MWT),[37] and vascular wall status (normal wall thickness/wall thickening/plaque formation) was evaluated independently, double-blindly, and the average of the two measurements was taken, as shown in Figure 2. Vascular wall status was determined by MWT based on previously validated and widely used thresholds in 3D HRMR-VWI research: < 1.0 mm was defined as normal (no evidence of arteriosclerosis), 1.0 to 1.5 mm as wall thickening (early arteriosclerotic change), and > 1.5 mm as plaque formation (indicating atherosclerosis).[38]

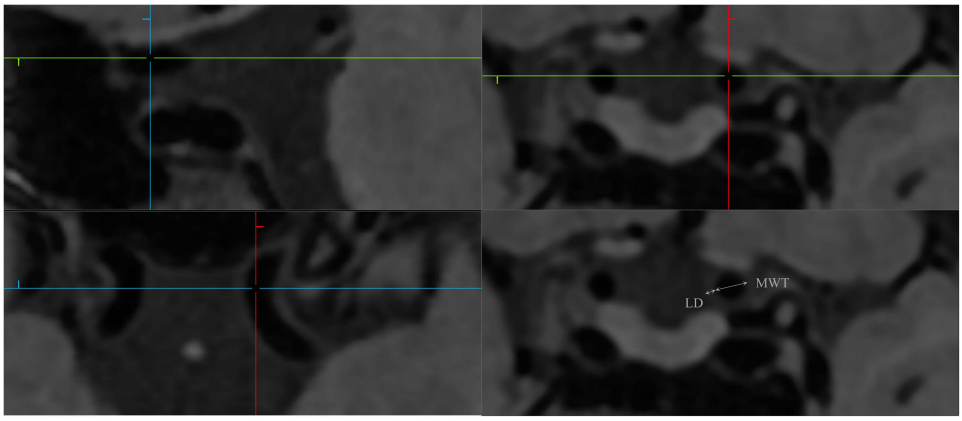

Figure 2 Schematic Diagram of Lumen Diameter (LD) and Maximum Wall Thickness (MWT) Measurement Using Multiplanar Reconstruction (MPR).

https://doi.org/10.2147/DMSO.S564173

Statistical Analysis

Data were analyzed using SPSS 27.0. Continuous variables were tested for normality (Shapiro–Wilk). Normally distributed data are expressed as mean ± SD; non-normal data are expressed as interquartile range (IQR). Categorical data are presented as n (%). Interobserver agreement was assessed using the two-way random-effects intraclass correlation coefficient (ICC(2,1)), a model appropriate for evaluating the agreement of single measurements obtained by two independent observers, and the widely accepted grading criteria for interobserver agreement in the field of clinical measurement were applied for interpretation: an ICC value ≥0.90 indicated excellent interobserver agreement, a value between 0.75 and 0.90 denoted good interobserver agreement, a value ranging from 0.40 to 0.75 represented moderate interobserver agreement, and an ICC value <0.40 meant poor interobserver agreement. Analysis of variance (ANOVA) (for normally distributed data) or Kruskal–Wallis H (for normally distributed data) tests were used for group comparisons, followed by LSD/Bonferroni post hoc tests. Trend χ^2 tests analyzed categorical variables. Ordinal logistic regression evaluated BMI (ordinal: 1=normal weight, 2=overweight, 3=obesity) and vessel wall status (1=normal vessel wall, 2=wall thickening, 3=plaque formation), validated by the Brant test. $p < 0.05$ is statistically significant, $p < 0.01$ is highly statistically significant, and $p < 0.001$ is very statistically significant.

Results

Clinical Characteristics of the Study Population

This study ultimately included 96 subjects (mean age 38.49 ± 8.97 years; 51.0% female, 49.0% male). A total of 1536 segments from 192 craniocervical arteries were analyzed via 3D HRMR-VWI. Demographics and clinical characteristics are shown in Table 1. No significant differences in age or gender were observed among BMI groups. The obese group had significantly higher levels of blood pressure (BP), CHO, LDL-C, TG, CR, UA, ALT, AST, and GGT than those of

Table 1 Demographic and Clinical Characteristics of Participants Across BMI Groups

Variable	Normal Weight (n=32)	Overweight (n=32)	Obesity (n=32)	*P*-value
Demographics				
Age (years)	38.03±7.46	38.53±10.31	38.81±9.18	0.940
Male Sex [n (%)]	15 (46.88%)	19 (59.4%)	13 (40.6%)	0.311
Anthropometrics				
Height (m)	1.63 (0.06)	1.59±0.08	1.69±0.09	0.006**
Weight (kg)	56.97±6.86	74.83±7.85	89.91±14.15	<0.01**
BMI (kg/m^2)	21.37 (3.89)	26.01 (2.26)	30.27 (5.10)	<0.01**
Lifestyle Factors				
Balanced Diet [n (%)]	22 (68.75%)	18 (56.25%)	10 (31.25%)	0.009**
Smoking status [n (%)]	5 (15.63%)	6 (18.75%)	10 (31.25%)	0.278
Insufficient sleep [n (%)]	3 (15.63%)	6 (18.75%)	7 (21.88%)	0.377
Regular Exercise [n (%)]	23 (71.88%)	16 (50%)	8 (25%)	<0.01**
Anamnesis				
Hypertension < 1year [n (%)]	2 (6.25%)	4 (12.5%)	5 (15.63%)	0.487
Diabetes < 1 year [n (%)]	1 (3.13%)	2 (6.25%)	4 (12.5%)	0.340
CAD < 1 year [n (%)]	0	1 (3.13%)	1 (3.13%)	0.600
Family history				
Father source [n (%)]	0	2 (6.25%)	5 (15.63%)	0.054
Mother source [n (%)]	0	1 (3.13%)	3 (9.38%)	0.161
Blood Pressure				
SBP (mmHg)	119.50 (6.75)	133.09±9.82	130.37±16.04	<0.01**
DBP (mmHg)	77.00 (7.75)	83.84±9.82	87.34±9.75	<0.01**

(*Continued*)

Table 1 (Continued).

Variable	Normal Weight (n=32)	Overweight (n=32)	Obesity (n=32)	*P*-value
Laboratory Indices				
Lipid Profile				
CHO (mmol/L)	4.39±0.93	4.94±0.91	5.19±0.86	0.002**
LDL-C (mmol/L)	2.27±0.64	2.90±0.76	2.92±0.68	<0.01**
HDL-C (mmol/L)	1.34±0.33	1.01 (0.32)	1.03±0.27	<0.01**
TG (mmol/L)	1.06 (0.8)	1.84 (1.05)	1.98 (1.23)	<0.01**
Renal Function Markers				
CR (μmol/L)	52.1±10.83	66.65 (21.32)	61.8±15.71	0.004**
UA (μmol/L)	273.5 (77.47)	365.1 (102.48)	394.08±88.29	<0.01**
Liver Enzymes				
ALT (U/L)	14.55 (9.20)	28.00 (27.28)	28.75 (25.35)	<0.01**
AST (U/L)	17.00 (4.75)	21.15 (11.00)	20.20 (7.13)	0.027*
GGT (U/L)	17.45 (18.88)	36.14±18.06	32.25 (23.30)	0.003**
Glucose Metabolism				
GLU (mmol/L)	5.08 (0.59)	5.85 (0.98)	5.75 (1.12)	<0.01**

Notes: Normal distribution: Mean ± SD; Non-normal distribution: Median (IQR).*p < 0.05, **p < 0.01.
Abbreviations: CAD, Coronary Artery Disease; BP, Blood pressure; SBP, systolic pressure; DBP, diastolic pressure; CHO, total cholesterol; LDL-C, low-density lipoprotein; HDL-C, high-density lipoprotein; TG, triglycerides; UA, uric acid; CR, creatinine; ALT, alanine aminotransferase; AST, aspartate aminotransferase; GGT, gamma-glutamyl transferase; GLU, glucose.

the overweight and normal weight groups ($P < 0.05$). Additionally, the obese group had lower rates of healthy diet and regular exercise ($P < 0.05$).

3D HRMR-VWI Comparison of Craniocervical Artery Segments Across BMI Groups

For the left ICA C6 segment randomly, inter-observer ICCs for LD and MWT were 0.94 (95% CI: 0.907–0.959) and 0.95 (95% CI: 0.925–0.967), indicating excellent consistency. As shown in Table 2, LD generally decreased from proximal to

Table 2 Comparison of Lumen Diameters (LD) of Different Segments of Carotid Arteries Across BMI Groups

Segment	Normal Weight	Overweight	Obesity	F/H Value	P-value
Left ICA C1	3.932±0.358	4.007±0.653	4.254±0.734	5.473^{H}	0.065
Left ICA C2	3.604±0.493	3.867±0.557	3.666±0.678	3.748^{H}	0.153
Left ICA C3	3.754±0.527	4.201±0.594	3.951±0.661	4.522^{F}	0.013*
Left ICA C4	4.145±0.493	4.255 (0.523)	4.262±0.686	2.476^{H}	0.290
Left ICA C5	3.692±0.448	4.043±0.643	3.767±0.541	3.624^{F}	0.031*
Left ICA C6	3.355±0.484	3.463±0.485	3.353±0.561	0.487^{F}	0.616
Left ICA C7	3.082±0.371	3.260±0.391	3.171±0.397	1.698^{F}	0.189
Left MCA M1	2.580 (0.413)	2.514±0.408	2.376±0.392	2.177^{H}	0.337
Right ICA C1	3.801±0.515	4.073±0.587	4.130 (0.720)	4.679^{H}	0.096
Right ICA C2	3.400±0.407	3.631±0.587	3.564±0.715	2.344^{H}	0.310
Right ICA C3	3.676±0.412	4.245±0.199	3.969±0.714	6.779^{F}	0.002**
Right ICA C4	4.152±0.570	4.278±0.580	4.082±0.746	0.779^{F}	0.462
Right ICA C5	3.963±0.628	3.824±0.596	3.9370±0.560	1.345^{F}	0.266
Right ICA C6	3.322±0.430	3.403±0.482	3.140 (0.450)	2.224^{H}	0.329
Right ICA C7	3.034±0.424	3.190±0.430	3.093±0.361	1.207^{F}	0.304
Right MCA M1	2.545 (0.360)	2.575±0.447	2.533±0.454	0.111^{H}	0.946

Notes: Normal distribution: Mean ± SD; Non-normal distribution: Median (IQR). The F-value is the analysis of variance (ANOVA); The H-value is the Kruskal–Wallis *H*-test. *p < 0.05, **p < 0.01.

https://doi.org/10.2147/DMSO.S564173

Table 3 Comparison of Maximum Wall Thickness (MWT) of Carotid Arteries in Different Segments Across BMI Groups

Artery Segment	Normal Weight	Overweight	Obesity	F/H Value	P-value
Left ICA C1	1.135 (0.443)	1.290 (0.440)	1.570 (0.630)	19.806^{H}	<0.001***
Left ICA C2	1.326±0.386	1.425 (0.658)	1.790 (0.875)	14.327^{H}	<0.001***
Left ICA C3	1.166±0.271	1.275 (0.372)	1.390 (0.410)	10.395^{H}	0.006**
Left ICA C4	1.070 (0.338)	1.296±0.286	1.305 (0.320)	6.784^{H}	0.034*
Left ICA C5	1.099±0.204	1.135 (0.350)	1.220 (0.590)	2.311^{H}	0.315
Left ICA C6	0.991±0.225	1.120 (0.343)	1.210 (0.410)	21.732^{H}	<0.001***
Left ICA C7	0.997±0.192	1.112±0.208	1.205±0.283	6.815^{F}	0.002**
Left MCA M1	0.897±0.233	0.967±0.229	1.049±0.255	3.187^{F}	0.046*
Right ICA C1	1.200 (0.208)	1.330 (0.328)	1.567±0.389	12.867^{H}	0.002**
Right ICA C2	1.265 (0.710)	1.540±0.479	1.860±0.592	10.152^{H}	0.006**
Right ICA C3	1.145±0.273	1.180 (0.480)	1.445 (0.480)	12.323^{H}	0.002**
Right ICA C4	1.075±0.215	1.185 (0.708)	1.295 (0.390)	13.316^{H}	0.001**
Right ICA C5	1.023±0.179	1.210±0.284	1.170 (0.450)	11.486^{H}	0.003**
Right ICA C6	1.069±0.250	1.107±0.208	1.184±0.245	1.917^{F}	0.153
Right ICA C7	0.995±0.192	1.101±0.217	1.201±0.148	3.375^{F}	0.041*
Right MCA M1	0.923±0.237	1.025±0.180	1.045 (0.300)	5.044^{H}	0.080

Notes: Normal distribution: Mean ± SD; Non-normal distribution: Median (IQR). The F-value is the analysis of variance (ANOVA); The H-value is the Kruskal–Wallis *H*-test. *p < 0.05, **p < 0.01, ***p < 0.001.

distal segments but slightly increased in C3-C4. The right C3 segment LD in the overweight group was significantly larger than in the normal weight group (overweight: 4.245 ± 0.199 mm vs normal weight: 3.676 ± 0.412 mm; $p < 0.01$), while the obese group showed retraction (obesity: 3.969 ± 0.714 mm, $p < 0.01$).

As shown in Table 3, MWT significantly thickened with increasing BMI (trend test: $Z = 10.99$, $P < 0.001$). The obese group had the most significant MWT increases in the left C1, C2, and C6 segments (H=19.806, 14.327, 21.732, $P < 0.001$) (examples in Figure 3). Differences in LD and MWT across segments are visualized in Figure 4.

Vessel Wall Status Distribution and Deterioration Risk

Vessel wall status (normal/thickening/plaque) differed significantly among BMI groups ($\chi^2 = 122.89$, $P <0.001$). Plaque detection rates were highest in the obese group (29.49%), followed by the overweight group (17.77%) and normal weight group (7.81%) ($P < 0.001$). Ordinal logistic regression (after validating the parallel lines assumption, $P = 0.145$) showed that each increase in BMI grade (normal weight → overweight → obesity) was associated with a 98% higher risk of vessel wall deterioration (OR = 1.98, 95% CI: 1.75–2.24, $P < 0.001$). Figure 5 illustrates the distribution of vessel wall status and OR estimates.

Discussion

This study revealed segment-specific remodeling of craniocervical lumen-wall structures in obese individuals combining 3D HRMR-VWI with Bouthillier segmentation: coexisting compensatory dilation and progressive thickening. The right ICA C3 segment (distal to the carotid sinus) dilated in the overweight group but retracted in the obese group, while the left C1 (carotid bulb), C2 (petrous segment), and C6 (ophthalmic segment) showed significant MWT thickening. This observation aligns with the "expansion-contraction" bidirectional remodeling theory.[39] In the early overweight stage, hemodynamic adaptations (eg, increased blood flow and shear stress triggered by metabolic changes) induce compensatory dilation of the right C3 segment, maintaining luminal patency to delay stenosis onset. However, with progressive obesity, persistent metabolic dysregulation (eg, lipotoxicity, chronic inflammation, and endothelial dysfunction) drives excessive collagen deposition and plaque formation, reducing vascular compliance and leading to luminal retraction in the obese group—marking a transition from compensatory to decompensatory remodeling.[3] The right C3 segment in obese individuals[40] is prone to hemodynamically significant atherosclerotic stenosis, causing abnormal post-stenotic

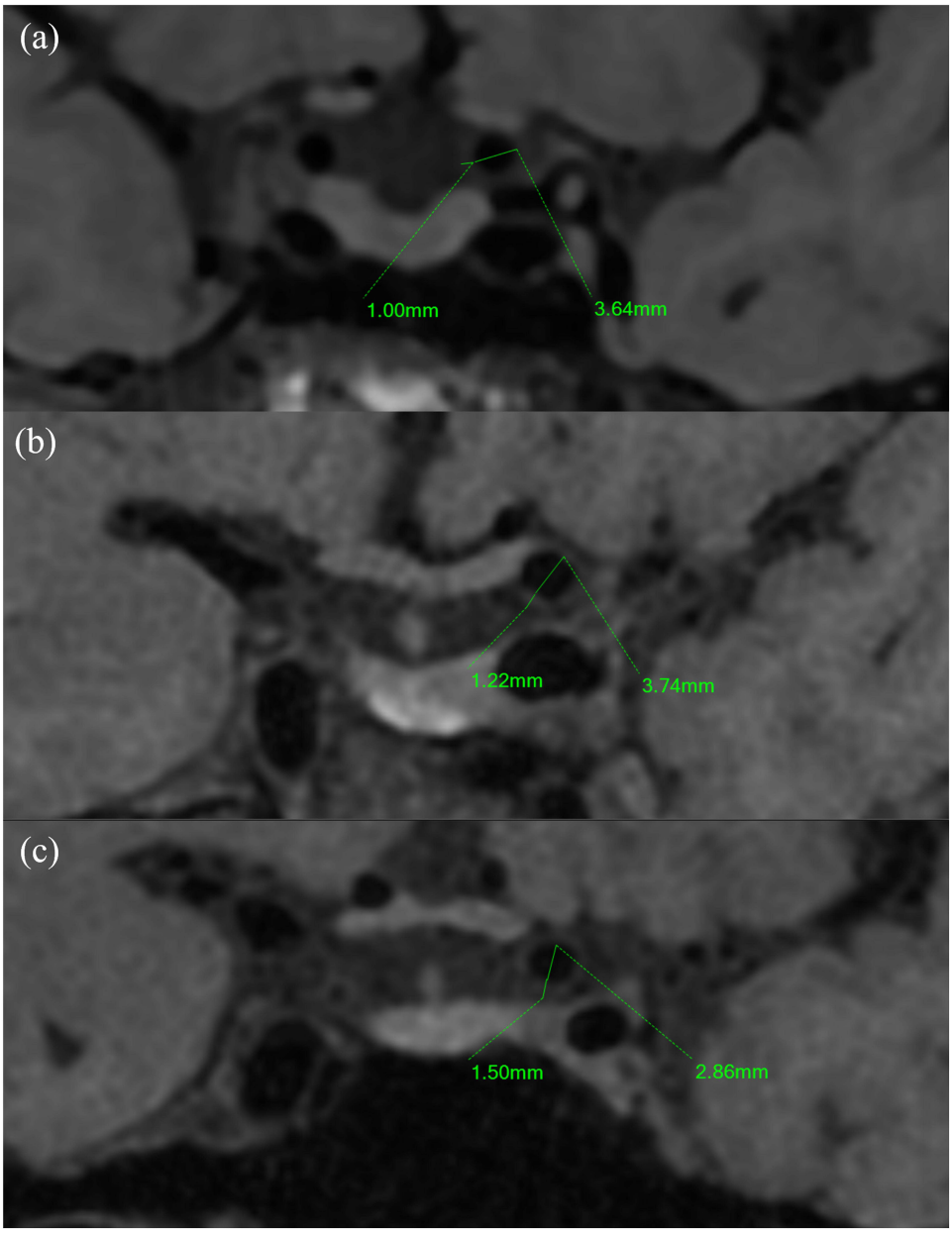

Figure 3 Example of Vessel Wall Status Comparison in Left ICA C6 Segment Across BMI Groups. (**a**) Normal weight group (BMI 19.56 kg/m^2); (**b**) Overweight group (BMI 26.89 kg/m^2); (**c**) Obesity group (BMI 34.55 kg/m^2).

hemodynamics[41] (low/oscillatory shear stress, turbulence, pressure gradients) and triggering reactive dilatory remodeling. Expansive remodeling is considered as a compensatory enlargement of the arterial wall during the progression of atherosclerosis, and is one of the hallmarks of vulnerable plaques. Unlike the singular expansion phenomenon observed in previous studies by Yoshida[42] and Yang,[43] our study suggests, through segmental quantification, that in obese populations there exists a bidirectional remodeling pattern characterized by concurrent craniocervical artery dilation and lumen narrowing due to wall thickening or plaque formation. These two phenomena may represent different stages of the disease (compensatory phase → decompensatory phase) and provide new evidence for positive remodeling theory.

Significant MWT thickening in the left C1, C2, and C6 segments of obese individuals may relate to anatomical differences: the left carotid artery originates from the aortic arch,[44] exposing the left common carotid artery and its branches (including the ICA origin) to greater pressure fluctuations and blood flow impact. High-velocity blood flow from the carotid bifurcation directly impacts the lateral walls of C1 (cervical segment) and C2 (petrous segment). The C6

https://doi.org/10.2147/DMSO.S564173

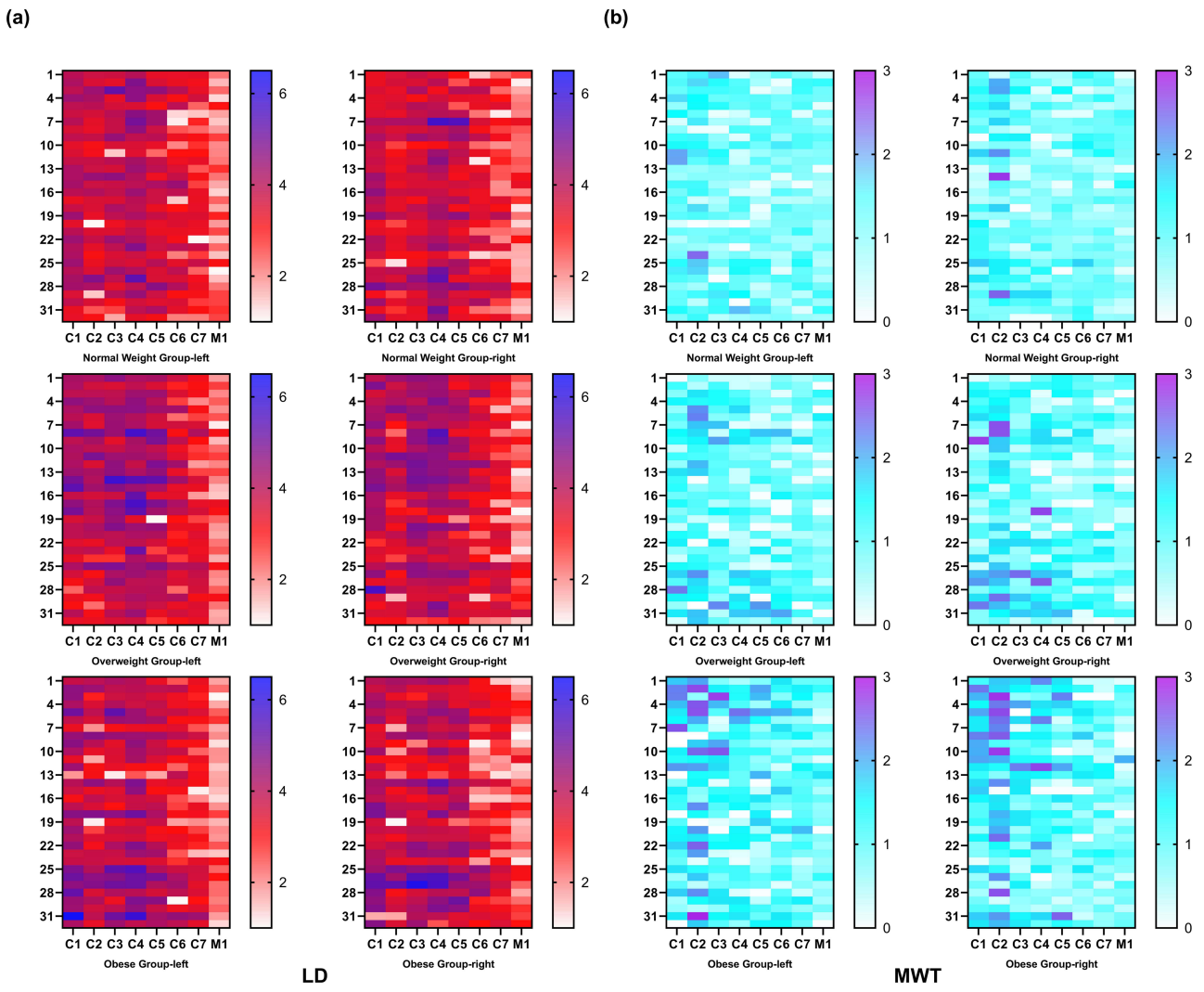

Figure 4 (**a**) Heatmap Visualization of Segmental Lumen Diameter (LD) Differences Across BMI Groups; (**b**) Heatmap Visualization of Segmental Maximum Wall Thickness (MWT) Differences Across BMI Groups.

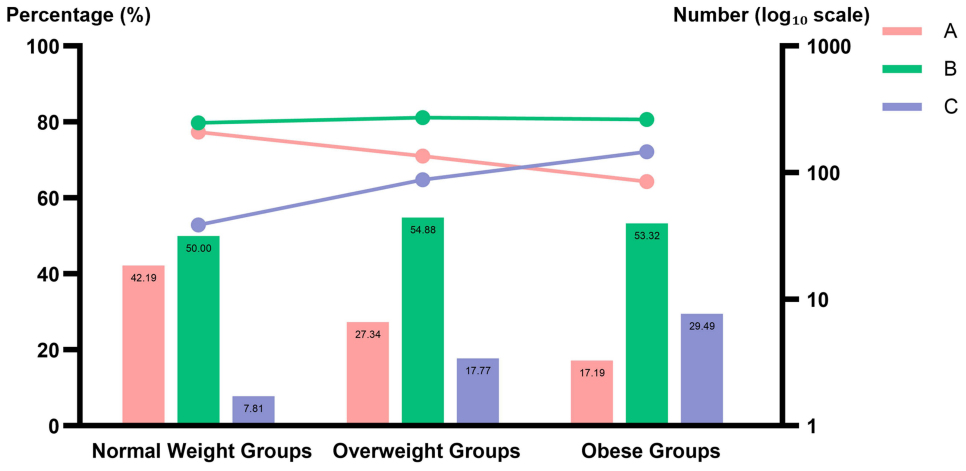

Figure 5 Odds Ratios for Vascular Wall Deterioration Across BMI Groups. A = normal vessel wall, B = wall thickening, C = plaque formation. Trend chi-square test (Z=10.99, χ^2=122.89, P < 0.001); ordinal logistic regression (OR=1.98, 95% CI: 1.75–2.24, P < 0.001).

https://doi.org/10.2147/DMSO.S564173

segment (ophthalmic segment) forms siphon bends within the cavernous sinus, where reduces flow velocity and turbulence at the inner walls and bifurcations lower shear stress, accelerating lipid deposition and inflammation. This view is consistent with the study of Damaskos.[45] However, Benson[46] suggested that internal carotid artery tortuosity was not related to carotid plaque composition and might not play a role in the development of high-risk plaques, possibly because their studies included symptomatic patients. However, our study included asymptomatic individuals with early-stage lesions, and the sensitivity of 3D HRMR-VWI to wall plaques is superior to that of traditional lumen imaging, resulting in a higher detection rate.

Furthermore, this study confirmed that each BMI grade increase (normal weight → overweight → obesity) raised the risk of plaque formation by 98%. Obese individuals had elevated free fatty acids, TG, LDL-C, UA, and liver enzymes, inducing lipotoxicity, oxidative stress, and chronic inflammation[4,8] that promoted endothelial dysfunction and matrix metalloproteinase activation. Lipid particles were prone to deposit in carotid bifurcations and curved segments (low shear stress areas), triggering monocyte differentiation into macrophages and foam cell formation, accelerating atherosclerosis.[47]

According to the latest research, the plaque rate in the normal BMI group was 7.8–8.3%, the overweight rate rose to 17.8–25.5%, and the obese group was as high as 29.5–45.3%.[48] Compared to our study, the specific values are different, but the specific data trends are consistent. These data further confirmed a significant positive correlation between BMI and cephalic carotid plaque. A general population cohort study based on the Korean community indicated that obesity increased the prevalence of carotid plaques compared to non-obese subjects.[49] Another study showed that obesity did not increase the risk of carotid atherosclerosis compared with metabolically healthy non-obese individuals.[50] They believed that metabolic health was a key factor in whether the risk of subclinical atherosclerosis increased, while our study used the 3D HRMR-VWI wall display technique, which showed that the wall thickness of the tube was more accurate than previous studies, which may be the main reason for the variability in the measurement results.

Our study had several limitations. First of all, the sample size of the single-center cross-sectional design of this study may be insufficient to establish the causal time sequence of BMI and vascular remodeling. It still needed to be verified by longitudinal follow-up whether the transition from expansion to retraction of the right C3 segment necessarily predicted lesion progression, and the universality of segmental remodeling needed to be verified by multicenter cohorts in the future. Secondly, although patients with a history of diabetes/hypertension > 1 year were excluded from this study, short-term metabolic fluctuations (such as acute elevation of blood glucose/blood lipids), lifestyle details (dietary sodium intake, exercise intensity) and inflammatory markers (such as hs-CRP, IL-6) were not continuously monitored, which may affect the results. In the future, continuous metabolic monitoring and lifestyle logs should be included, and artificial intelligence should be used to analyze multimodal data to improve the accuracy of the model. Finally, there might be measurement errors between observers in this study, caused by manual measurement, and image segmentation technology will be used to provide measurement accuracy in the future.

Conclusion

This study utilizes 3D HRMR-VWI technology to reveal segment-specific remodeling of cerebral blood vessels in obese populations: the dilation of the right C3 segment may indicate early compensatory remodeling, while the thickening of the left C1, C2, and C6 segments suggests progressive lesions. Elevated BMI dose-dependently increases vessel wall deterioration risk. These findings provide new evidence for optimizing 3D HRMR-VWI screening strategies (focusing on high-risk segments) and for establishing BMI stratification intervention thresholds.

Data Sharing Statement

Data are available upon request from the corresponding author.

Statement of Ethics

This study was performed in accordance with the Declaration of Helsinki. This human study was approved by Qinhuangdao NO.1 Hospital - approval: No. 2025K-250-01. All adult participants provided written informed consent to participate in this study. Written informed consent was obtained from the individual(s) for publication of the details of their medical case and any accompanying images.

Author Contributions

Ai Li, Jun Zhang and Hongtao Niu: conceptualization, data curation, formal analysis, investigation, methodology, validation, writing - original draft, and writing - review and editing; Ai Li, Miao Yu, Fei Wang, Qiang Lu: data curation, formal analysis, investigation, methodology, validation, writing - original draft, and writing - review and editing. All authors gave final approval of the version to be published; have agreed on the journal to which the article has been submitted and agree to be accountable for all aspects of the work.

Funding

This work was supported by the S&T Program of Qinhuangdao (Grant No.: 202501A099).

Disclosure

All authors declare no conflicts of interest in this work.

References

1. World Health Organization. News-room fact-sheets detail obesity and overweight [Online]. 2020. Available from: https://www.who.int/newsroom/fact-sheets/detail/obesity-and-overweight. Accessed February 18, 2026.
2. Feigin VL, Stark BA, Johnson CO, et al. Global, regional, and national burden of stroke and its risk factors, 1990–2019: a systematic analysis for the Global Burden of Disease Study 2019. *Lancet Neurol*. 2021;20(10):795–820. doi:10.1016/S1474-4422(21)00252-0
3. Bondareva O, Rodríguez-Aguilera JR, Oliveira F, et al. Single-cell profiling of vascular endothelial cells reveals progressive organ-specific vulnerabilities during obesity. *Nat Metab*. 2022;4(11):1591–1610. doi:10.1038/s42255-022-00674-x
4. Adam S, Maas SL, Huchzermeier R, et al. The calcium-sensing-receptor (CaSR) in adipocytes contributes to sex-differences in the susceptibility to high fat diet induced obesity and atherosclerosis. *eBioMedicine*. 2024;107:105293. doi:10.1016/j.ebiom.2024.105293
5. Kim D, Memili A, Chen HH, et al. Sex-specific associations between adipokine profiles and carotid-intima media thickness in the Cameron County Hispanic Cohort (CCHC). *Cardiovasc Diabetol*. 2023;22(1). doi:10.1186/s12933-023-01968-4
6. Fico BG, Miller KB, Rivera-Rivera LA, et al. Cerebral hemodynamics comparison using transcranial Doppler ultrasound and 4D flow MRI. *Front Physiol*. 2023;14. doi:10.3389/fphys.2023.1198615
7. Fresilli D, Di Leo N, Martinelli O, et al. 3D-Arterial analysis software and CEUS in the assessment of severity and vulnerability of carotid atherosclerotic plaque: a comparison with CTA and histopathology. *La radiologia medica*. 2022;127(11):1254–1269. doi:10.1007/s11547-022-01551-z
8. Denis L, Meseguer E, Gaudemer A, et al. Transcranial ultrasound localization microscopy in moyamoya patients using a clinical ultrasound system. *Theranostics*. 2025;15(9):4074–4083. doi:10.7150/thno.105427
9. Luo J, Bai X, Huang K, et al. Clinical relevance of plaque distribution for Basilar artery stenosis. *Am J Neuroradiol*. 2023;44(5):530–535. doi:10.3174/ajnr.A7839
10. Wan M, Yan L, Xu Z, et al. Symptomatic and asymptomatic chronic carotid artery occlusion on high-resolution MR vessel wall imaging. *Am J Neuroradiol*. 2021;43(1):110–116. doi:10.3174/ajnr.A7365
11. Mantella LE, Liblik K, Johri AM. Vascular imaging of atherosclerosis: strengths and weaknesses. *Atherosclerosis*. 2021;319:42–50. doi:10.1016/j.atherosclerosis.2020.12.021
12. Arslan S, Korkmazer B, Kizilkilic O. Intracranial vessel wall imaging. *Curr Opin Rheumatol*. 2021;33(1):41–48. doi:10.1097/BOR.0000000000000759
13. Kang DW, Kim DY, Kim J, et al. Emerging concept of intracranial arterial diseases: the role of high resolution vessel wall MRI. *J Stroke*. 2024;26(1):26–40. doi:10.5853/jos.2023.02481
14. Bouthillier A, van Loveren HR, Keller JT. Segments of the Internal Carotid Artery: a New Classification. *Neurosurgery*. 1996;38(3):425–433. doi:10.1097/00006123-199603000-00001
15. Zhang F, Yao H, Langzam E, et al. Detectability of intracranial vessel wall atherosclerosis using black-blood spectral CT: a phantom and clinical study. *Eur Radiol Exp*. 2024;8(1). doi:10.1186/s41747-024-00473-x
16. Engelter ST, Lyrer P, Traenka C. Cervical and intracranial artery dissections. *Ther Adv Neurol Disord*. 2021;14. doi:10.1177/17562864211037238
17. Ihara M, Yamamoto Y, Hattori Y, et al. Moyamoya disease: diagnosis and interventions. *Lancet Neurol*. 2022;21(8):747–758. doi:10.1016/S1474-4422(22)00165-X
18. Niemann A, Tulamo R, Netti E, et al. Multimodal exploration of the intracranial aneurysm wall. *Int J Comput Assist Radiol Surg*. 2023;18(12):2243–2252. doi:10.1007/s11548-023-02850-0
19. Yang Y, Hua Y, Jia L. Relationship between carotid artery remodeling characteristics and early carotid atherosclerosis. *J Ultrasound Med*. 2025;44(5):915–925. doi:10.1002/jum.16651
20. Espitia O, Robin O, Hersant J, et al. Inter and intra-observer agreement of arterial wall contrast-enhanced ultrasonography in giant cell arteritis. *Front Med*. 2022;9. doi:10.3389/fmed.2022.1042366
21. Wang Y, Yuan T, Deng S, et al. Metabolic health phenotype better predicts subclinical atherosclerosis than body mass index-based obesity phenotype in the non-alcoholic fatty liver disease population. *Front Nutr*. 2023;10. doi:10.3389/fnut.2023.1104859
22. Wang Y, Li L, Li Y, et al. The impact of dietary diversity, lifestyle, and blood lipids on carotid atherosclerosis: a cross-sectional study. *Nutrients*. 2022;14(4):815. doi:10.3390/nu14040815
23. Lu Y, Pechlaner R, Cai J, et al. Trajectories of age-related arterial stiffness in Chinese men and women. *Journal of the American College of Cardiology*. 2020;75(8):870–880. doi:10.1016/j.jacc.2019.12.039
24. Xue J, Allaband C, Zuffa S, et al. Gut microbiota and derived metabolites mediate obstructive sleep apnea induced atherosclerosis. *Gut Microbes*. 2025;17(1). doi:10.1080/19490976.2025.2474142

25. Feske SK. Ischemic Stroke. *Am J Med*. 2021;134(12):1457–1464. doi:10.1016/j.amjmed.2021.07.027
26. Wang X, Chen H, Chang Z, Zhang J, Xie D. Genetic causal role of body mass index in multiple neurological diseases. *Sci Rep*. 2024;14(1):7256.
27. Weyand CM, Goronzy JJ. Immunology of giant cell arteritis. *Circ Res*. 2023;132(2):238–250. doi:10.1161/CIRCRESAHA.122.322128
28. Li H, Song P, Yang W, et al. Association between autoimmune diseases and spontaneous cervicocranial arterial dissection. *Front Immunol*. 2022;12. doi:10.3389/fimmu.2021.820039
29. Hankard A, Maalouf G, Laouni J, et al. Outcome and prognosis of isolated carotid vasculitis. *J Autoimmun*. 2024;146:103242. doi:10.1016/j.jaut.2024.103242
30. Kriemler L, Rudin S, Gawinecka J, et al. Discordance between LDL-C and apolipoprotein B is associated with large-artery-atherosclerosis ischemic stroke in patients ⩽70 years of age. *Eur Stroke J*. 2024;9(2):494–500. doi:10.1177/23969873231221619
31. Ferraro S, Benedetti S, Mannarino S, Marcovina S, Mario Biganzoli E, Zuccotti G. Prediction of atherosclerotic cardiovascular risk in early childhood. *Clin Chim Acta*. 2024;552:117684. doi:10.1016/j.cca.2023.117684
32. Kanmiki EW, Fatima Y, Mamun AA. Multigenerational transmission of obesity: a systematic review and meta-analysis. *Obesity Rev*. 2021;23(3):e13405.
33. Pan XF, Wang L, Pan A. Epidemiology and determinants of obesity in China. *Lancet Diabetes Endocrinol*. 2021;9(6):373–392.
34. Ma Y, Wang M, Qiao Y, et al. Feasibility of artificial intelligence constrained compressed SENSE accelerated 3D Isotropic T1 vista sequence for vessel wall MR imaging: exploring the potential of higher acceleration factors compared to traditional compressed SENSE. *Acad Radiol*. 2024;31(10):3971–3981. doi:10.1016/j.acra.2024.03.041
35. Nie Y, Lu N, Liao L, et al. Black-blood magnetization prepared 2 rapid acquisition gradient Echoes: a fast and three-dimensional MR Black-Blood T_1 mapping technique for quantitative assessment of atherosclerosis and venous thrombosis. *J Magn Reson Imaging*. 2023;60(3):1148–1162. doi:10.1002/jmri.29156
36. Bevan JA, Dodge J, Walters CL, Wellman T, Bevan RD. As human pial arteries (internal diameter 200–1000 μm) get smaller, their wall thickness and capacity to develop tension relative to their diameter increase. *Life Sci*. 1999;65(11):1153–1161. doi:10.1016/S0024-3205(99)00349-5
37. Cui Z, Xu S, Miu J, et al. Development and validation of a fusion model based on carotid plaques and white matter lesion burden imaging characteristics to evaluate ischemic stroke severity in symptomatic patients. *J Magn Reson Imaging*. 2024;61(2):648–660. doi:10.1002/jmri.29439
38. Yu M, Zhang S, Wang L, Wu J, Li X, Yuan J. Metabolically healthy obesity and carotid plaque among steelworkers in North China: the role of inflammation. *Nutrients*. 2022;14(23):5123. doi:10.3390/nu14235123
39. Koskinas KC, Maldonado R, Garcia-Garcia HM, et al. Relationship between arterial remodelling and serial changes in coronary atherosclerosis by intravascular ultrasound: an analysis of the IBIS-4 study. *Eur Heart J Cardiovasc Imaging*. 2020;22(9):1054–1062. doi:10.1093/ehjci/jeaa221
40. Wu Y, Dai Y, Jia Y, Yu S, Xu S, Wang W. Carotid artery plaques and unilateral spatial neglect in the elderly. *Medicine*. 2020;99(4):e18998. doi:10.1097/MD.0000000000018998
41. Mendieta JB, Fontanarosa D, Wang J, et al. MRI-based mechanical analysis of carotid atherosclerotic plaque using a material-property-mapping approach. *Comput Methods Programs Biomed*. 2023;231:107417. doi:10.1016/j.cmpb.2023.107417
42. Yoshida K, Yang T, Yamamoto Y, et al. Expansive carotid artery remodeling: possible marker of vulnerable plaque. *J Neurosurg*. 2020;133(5):1435–1440. doi:10.3171/2019.7.JNS19727
43. Yang W, Sam K, Qiao Y, Huang Z, Steinman DA, Wasserman BA. A novel window into human vascular remodeling and diagnosing carotid flow impairment: the petro-occipital venous plexus. *J Am Heart Assoc*. 2023;12(20):031832. doi:10.1161/JAHA.123.031832
44. Kim HJ, Song JM, Kwon SU, et al. Right–left propensity and lesion patterns between cardiogenic and aortogenic cerebral embolisms. *Stroke*. 2011;42(8):2323–2325. doi:10.1161/STROKEAHA.111.616573
45. Damaskos S, da Silveira HLD, Berkhout EWR. Severity and presence of atherosclerosis signs within the segments of internal carotid artery: CBCT's contribution. *Oral Surg Oral Med Oral Pathol Oral Radiol*. 2016;122(1):89–97. doi:10.1016/j.oooo.2016.03.017
46. Benson JC, Shahid A, Larson A, et al. Carotid artery tortuosity and internal carotid artery plaque composition. *Clin Neuroradiol*. 2023;33(4):1017–1021. doi:10.1007/s00062-023-01302-1
47. Ray M, Autieri MV. Regulation of pro- and anti-atherogenic cytokines. *Cytokine*. 2019;122:154175. doi:10.1016/j.cyto.2017.09.031
48. Zeng Q, Zhang C, Liu X, et al. Prevalence and associated risk factors of carotid plaque and artery stenosis in China: a population-based study. *Front Med*. 2024;19(1):64–78. doi:10.1007/s11684-024-1088-0
49. Itoh H, Kaneko H, Kiriyama H, et al. Effect of metabolically healthy obesity on the development of carotid plaque in the general population: a community-based cohort study. *J Atheroscler Thromb*. 2020;27(2):155–163. doi:10.5551/jat.48728
50. Seo DH, Cho Y, Seo S, et al. Association between metabolically healthy obesity and subclinical atherosclerosis in the Cardiovascular and Metabolic Diseases Etiology Research Center (CMERC) Cohort. *J Clin Med*. 2022;11(9):2440. doi:10.3390/jcm11092440